

# Signatures of the chiral anomaly in phonon dynamics

P. Rinkel, P. L. S. Lopes, and Ion Garate

*Département de Physique, Institut Quantique and Regroupement Québécois sur les Matériaux de Pointe,  
Université de Sherbrooke, Sherbrooke, Québec, Canada J1K 2R1*

(Dated: June 27, 2022)

Discovered in high-energy physics, the chiral anomaly has recently made way to materials science by virtue of Weyl semimetals. Thus far, the main efforts to probe the chiral anomaly in quantum materials have concentrated on electronic phenomena. Here, we show that the chiral anomaly can have a notable impact in phonon properties, including phonon dispersion, infrared absorption, and Raman scattering. Remarkably, in enantiomorphic Weyl semimetals, the chiral anomaly leads to a magnetically induced effective phonon charge with an unusual and potentially measurable resonance.

PACS numbers:

*Introduction.*— A major recent development in quantum materials has been the discovery of three dimensional semimetals containing Weyl nodes, i.e. topologically robust points of contact in momentum space between two nondegenerate and linearly-dispersing electronic bands [1]. These so-called Weyl semimetals (WSM) have low-energy properties governed by pairs of massless chiral fermions (Weyl fermions) of opposite chirality. The action for one such pair reads [2]

$$S_e = \int dt d^3\mathbf{r} \bar{\psi} (i\gamma^\mu \partial_\mu - \gamma^\mu A_\mu - \gamma^5 \gamma^\mu b_\mu) \psi, \quad (1)$$

where  $\mathbf{r}$  and  $t$  are space and time,  $\mu \in \{t, x, y, z\}$ ,  $\partial_\mu = (\partial_t, v\nabla)$ ,  $v$  is the Fermi velocity,  $\psi$  and  $\bar{\psi}$  are Dirac spinors,  $\gamma^\mu = (\tau^x, i\tau^y\boldsymbol{\sigma})$  and  $\gamma^5 = \tau^z$  are Dirac matrices,  $\tau^z$  labels the two Weyl nodes,  $\sigma^z$  labels the two degenerate states at each node,  $A^\mu = (e\phi, -e\mathbf{v}\mathbf{A})$  is the electromagnetic potential (the constant and uniform part of  $e\phi$  can be identified with the Fermi energy  $\epsilon_F$ ),  $e$  is the electron's charge and  $b_\mu = (b_0, \mathbf{b})$  is the axial vector describing the separation between the Weyl nodes in energy and momentum space ( $b_0$  and  $\mathbf{b}$ , respectively). We take  $\hbar \equiv 1$  throughout unless otherwise stated.

A key topological phenomenon in WSM is the chiral anomaly, by which collinear electric and magnetic fields induce a transfer of electrons between Weyl nodes of opposite chirality. The chiral anomaly enforces an unusual electromagnetic response in WSM [1, 3], which has been probed via electronic transport experiments [4]. Alternative probes, however, could provide complementary understanding of this phenomenon, and as such are much sought after [5–7]. Phonons are promising candidates in this search because they are ubiquitously coupled to electrons and can be accurately measured.

Recent theories hint at an interesting interplay between lattice vibrations and electronic topology: phonons can induce topological phase transitions [8], band inversions leave fingerprints in phonon linewidths [9], Hall viscosity impacts acoustic phonons [10], and strain can produce chiral gauge fields [11, 12]. Yet, to date, phonon measurements have found no evidence of topological ef-

fects [13], in part due to a scarcity of concrete theoretical ideas on what to measure. The objective of this work is to predict direct signatures of the chiral anomaly in phonon dynamics, infrared absorption and Raman scattering.

*Lattice dynamics in the absence of electrons.*— We begin by considering a crystal of volume  $\mathcal{V}$  with  $N$  unit cells and  $r$  atoms per unit cell. An atom  $s$  in unit cell  $\mathbf{l}$  has a mass  $M_s$ , an ionic charge  $eZ_s$  and an equilibrium position  $\mathbf{R}(\mathbf{l}, s) = \mathbf{l} + \mathbf{t}_s$ . Let  $\mathbf{w}_{\mathbf{l}s}(t)$  be the displacement of this atom away from its equilibrium position at time  $t$ . Ignoring electrons, the dynamics of small lattice vibrations is obtained from the action [14]

$$S^{(0)} = \int \frac{dq_0}{2\pi} \sum_{\mathbf{q}\lambda} \left[ \frac{1}{2} M(q_0^2 - \omega_{\mathbf{q}\lambda}^2) |v_{\mathbf{q}\lambda}(q_0)|^2 + \mathbf{A}_{\mathbf{q}}(q_0) \cdot \mathbf{j}_{-\mathbf{q}}(-q_0) - \phi_{\mathbf{q}}(q_0) \rho_{-\mathbf{q}}(-q_0) \right], \quad (2)$$

where  $q_0$  and  $\mathbf{q}$  are the frequency and the wave vector,  $M = \sum_s M_s$  is the total mass in a unit cell,

$$v_{\mathbf{q}\lambda}(q_0) = \frac{1}{\sqrt{N}} \sum_{\mathbf{l}s} e^{-i\mathbf{q}\cdot\mathbf{l}} \frac{M_s}{M} \mathbf{p}_{-\mathbf{q}\lambda s} \cdot \mathbf{w}_{\mathbf{l}s}(q_0) \quad (3)$$

is the normal mode coordinate,  $\lambda = 1, \dots, 3r$  is the normal mode index,  $\omega_{\mathbf{q}\lambda}$  are the normal mode frequencies in the absence of electromagnetic fields,  $\mathbf{p}_{\mathbf{q}\lambda s}$  is the polarization vector describing the motion of atom  $s$  in the mode  $(\lambda, \mathbf{q})$ , and  $\mathbf{j}(\rho)$  is the current (charge) density resulting from lattice vibrations. Then,  $\delta S^{(0)}/\delta v_{\mathbf{q}\lambda}(q_0) = 0$  yields

$$M(q_0^2 - \omega_{\mathbf{q}\lambda}^2) v_{\mathbf{q}\lambda}(q_0) = \sqrt{N} \mathbf{Q}_{\mathbf{q}\lambda}^{(0)} \cdot \mathbf{E}_{\mathbf{q}}(q_0), \quad (4)$$

where  $\mathbf{E}_{\mathbf{q}}(q_0)$  is the electric field in  $(q_0, \mathbf{q})$  space and

$$\mathbf{Q}_{\mathbf{q}\lambda}^{(0)} = e \sum_s Z_s e^{-i\mathbf{q}\cdot\mathbf{t}_s} \mathbf{p}_{\mathbf{q}\lambda s} \quad (5)$$

is the effective phonon charge vector associated with mode  $\lambda$ , i.e. the projection of Born effective charges onto the mode  $\lambda$  [15]. In the long-wavelength limit, Eq. (5) describes the change in the intracell electric polarization produced by atomic displacements in mode  $\lambda$ . The mode is infrared (IR) active if  $Q_{\mathbf{q}\lambda}^{(0)} \neq 0$ , IR inactive otherwise.

*Electron-phonon interaction.*— The lattice potential of the crystal in equilibrium is  $U(\mathbf{r}) = \sum_{\mathbf{l}s} U_s(\mathbf{r} - \mathbf{R}(\mathbf{l}, s))$ . The departures of the atoms from their equilibrium positions produce a change in  $U(\mathbf{r})$ ,  $\delta U(\mathbf{r}, t) \simeq \sum_{\mathbf{l}s} \mathbf{w}_{\mathbf{l}s}(t) \cdot [\partial U_s(\mathbf{r} - \mathbf{R}(\mathbf{l}, s))/\partial \mathbf{R}(\mathbf{l}, s)]$ , which couples locally to the electronic density operator  $\rho(\mathbf{r}) = \psi^\dagger(\mathbf{r})\psi(\mathbf{r})$ :

$$\mathcal{H}_{\text{ep}} = \int d^3\mathbf{r} \rho(\mathbf{r}) \delta U(\mathbf{r}, t). \quad (6)$$

Limiting ourselves to electronic states in the vicinity of Weyl nodes and adopting the Kohn-Luttinger representation [16], we have

$$\psi(\mathbf{r}) \simeq \frac{1}{\sqrt{\mathcal{V}}} \sum_{\tau} e^{i\mathbf{k}_\tau \cdot \mathbf{r}} \sum_{|\mathbf{k}| < \Lambda, \sigma} e^{i\mathbf{k} \cdot \mathbf{r}} u_{\sigma\tau}(\mathbf{r}) c_{\mathbf{k}\sigma\tau}, \quad (7)$$

where  $\mathbf{k}_\tau$  is the position of node  $\tau$  in momentum space,  $u_{\sigma\tau}(\mathbf{r}) \equiv u_{\mathbf{k}_\tau, \sigma}(\mathbf{r})$  is the periodic part of the Bloch wave function at node  $\tau$ ,  $\mathbf{k}$  is the momentum measured from a Weyl node, and  $\Lambda$  is a high momentum cutoff (smaller than the internode separation in  $\mathbf{k}$  space). Substituting Eq. (7) in Eq. (6) and inverting Eq. (3), we obtain

$$\mathcal{H}_{\text{ep}}^{\text{loc}} = \sum_{\mathbf{k}\mathbf{q}} \sum_{\sigma\sigma'\tau\tau'} g_{\sigma\tau, \sigma'\tau'}(\mathbf{q}, t) c_{\mathbf{k}\sigma\tau}^\dagger c_{\mathbf{k}-\mathbf{q}+\mathbf{k}_\tau-\mathbf{k}_{\tau'}\sigma'\tau'}, \quad (8)$$

where  $|\mathbf{k}| < \Lambda$ ,  $|\mathbf{k} - \mathbf{q} + \mathbf{k}_\tau - \mathbf{k}_{\tau'}| < \Lambda$ , and

$$g_{\sigma\tau, \sigma'\tau'}(\mathbf{q}, t) = \frac{\sqrt{N}}{\mathcal{V}} \sum_{\lambda s} v_{\mathbf{q}\lambda}(t) \mathbf{p}_{\mathbf{q}\lambda s} \cdot \int d^3\mathbf{r} e^{-i\mathbf{q} \cdot \mathbf{r}} u_{\sigma\tau}^*(\mathbf{r}) u_{\sigma'\tau'}(\mathbf{r}) \frac{\partial U_s(\mathbf{r} - \mathbf{R}(\mathbf{0}, s))}{\partial \mathbf{R}(\mathbf{0}, s)}. \quad (9)$$

Hereafter, we will be interested in long wavelength phonons ( $|\mathbf{q}| \ll |\mathbf{k}_\tau - \mathbf{k}_{\tau'}|$  for  $\tau \neq \tau'$ ), which are unable to scatter electrons between different nodes. It is then convenient to decompose

$$g_{\sigma\tau, \sigma'\tau'}(\mathbf{q}, q_0) = \delta_{\tau\tau'} \sum_{i=0}^3 [g_{i0} \sigma_{\sigma\sigma'}^i + g_{iz} \sigma_{\sigma\sigma'}^i \tau], \quad (10)$$

where  $\sigma^i$  are Pauli matrices ( $\sigma^0 = \mathbf{1}$ ),  $g_{i0} = \sum_{\sigma\sigma'\tau} \sigma_{\sigma\sigma'}^i g_{\sigma\tau, \sigma'\tau}/4$  and  $g_{iz} = \sum_{\sigma\sigma'\tau} \sigma_{\sigma\sigma'}^i \tau g_{\sigma\tau, \sigma'\tau}/4$ . Physically,  $g_{00}$  and  $\mathbf{g}_z = (g_{xz}, g_{yz}, g_{zz})$  describe phonon-induced vector fields, coupled to electrons. Similarly,  $g_{0z}$  and  $\mathbf{g}_0 = (g_{x0}, g_{y0}, g_{z0})$  are phonon-induced axial-vector fields: they produce oscillations in the energy difference and momentum separation between Weyl nodes of opposite chirality, respectively.

While  $g_{00}$  is generally allowed by symmetry,  $g_{0z} \neq 0$  requires  $\sum_{\tau} |u_{\sigma\tau}(\mathbf{r})|^2 \tau \neq 0$ , which in turn demands a WSM belonging to an enantiomorphic point group (broken inversion and mirror symmetries). SrSi<sub>2</sub> [17], as well as trigonal Se and Te [18], are candidate enantiomorphic WSM. Similarly,  $\mathbf{g}_z \neq 0$  requires broken time-reversal (TR), inversion and mirror symmetries, while

$\mathbf{g}_0 \neq 0$  requires breaking of TR symmetry. From the microscopic point of view, cf. Eq. (9),  $\mathbf{g}_z = \mathbf{g}_0 = 0$  because the band touching at each Weyl node implies  $\sum_{\sigma} \sigma |u_{\sigma\tau}(\mathbf{r})|^2 = 0$ . However, a more realistic treatment of the electronic structure [19] going beyond Eq. (7) could result in nonzero  $\mathbf{g}_z$  and  $\mathbf{g}_0$ .

In general, Weyl nodes are located at arbitrary points in the Brillouin zone, where the Bloch states transform according to a one dimensional irreducible representation (irrep) of the translation subgroup. Accordingly [20], only phonons that transform as the totally symmetric irrep ( $A_1$ ) contribute to  $g_{i0}$  and  $g_{iz}$ . In enantiomorphic crystals,  $A_1$  phonons are pseudoscalar.

*Phonon dynamics in presence of electrons.*— Electrons in WSM modify the effective action for phonons from  $S^{(0)}$  to  $S = S^{(0)} + S_{\text{int}}$ , where

$$S_{\text{int}} = -i \ln \det (i\gamma^\mu \partial_\mu - \gamma^\mu A_\mu - \gamma^5 \gamma^\mu a_\mu), \quad (11)$$

$a_\mu = b_\mu + (g_{0z}, \mathbf{g}_0)$  is the dynamical axial vector, and  $A_\mu$  contains a phonon-dependent part ( $g_{00}, \mathbf{g}_z$ ). Our next goal is to evaluate the phonon dynamics from  $\delta S/\delta v_{\mathbf{q}\lambda} = 0$  and to understand the impact of the chiral anomaly. We proceed by expanding  $S_{\text{int}} = S_2 + S_3 + \dots$  in powers of  $A^\mu$  and  $a^\mu$ , where

$$S_2 = \int_q \Pi_{\mu\nu}(q) [A^\mu(q) A^\nu(-q) + a^\mu(q) a^\nu(-q)]$$

$$S_3 = \int_{k,k'} T_{\alpha\mu\nu}(k, k') A^\mu(k) A^\nu(k') a^\alpha(-k - k'), \quad (12)$$

$k^\mu = (k_0, v\mathbf{k})$  and  $\int_k \equiv \int d^4k/(2\pi)^4 \simeq v^3/(2\pi\mathcal{V}) \sum_{\mathbf{k}} \int dk_0$ . Terms with an odd number of  $A^\mu$  vanish in presence of charge conjugation symmetry ( $\epsilon_F = 0$ ), which we assume for the sake of simplicity. We concentrate on terms that are *first-order* in  $g_{\sigma\tau\sigma'\tau'}$ , describing the impact of electric  $\mathbf{E}$  or magnetic fields  $\mathbf{B}$  in the phonon dynamics. Thus, in  $S_3$ , we have neglected a term involving  $a^\mu(k) a^\nu(k') a^\alpha(-k - k')$ .

Gauge invariance dictates  $\Pi_{\mu\nu}(q) = (q^2 g_{\mu\nu} - q_\mu q_\nu) \Pi(q^2)$ , where  $q^2 = q_0^2 - v^2 |\mathbf{q}|^2$  and  $\Pi(q^2)$  is the polarization function. It follows that

$$S_2 \simeq - \sum_{\mathbf{q}\lambda} \int \frac{dq_0}{2\pi} \sqrt{N} v_{\mathbf{q}\lambda}(q_0) \left[ \mathbf{Q}_{\mathbf{q}\lambda}^{(1)}(q_0) \cdot \mathbf{E}_{-\mathbf{q}}(-q_0) + v \mathbf{Q}_{\mathbf{q}\lambda}^{(2)}(q_0) \cdot \mathbf{B}_{-\mathbf{q}}(-q_0) \right], \quad (13)$$

where we have omitted pure phonon (photon) terms, and

$$\mathbf{Q}_{-\mathbf{q}\lambda}^{(1)}(-q_0) = \frac{ie\mathcal{V}}{\hbar v^2 \sqrt{N}} \Pi(q^2) \frac{\partial}{\partial v_{\mathbf{q}\lambda}(q_0)} (q_0 \mathbf{g}_z - v \mathbf{q} g_{00})$$

$$\mathbf{Q}_{-\mathbf{q}\lambda}^{(2)}(-q_0) = \frac{ie\mathcal{V}}{\hbar v^2 \sqrt{N}} \Pi(q^2) \frac{\partial}{\partial v_{\mathbf{q}\lambda}(q_0)} (v \mathbf{q} \times \mathbf{g}_z) \quad (14)$$

are vectors describing the electronic contribution to the phonon effective charge and to an extra  $\mathbf{B}$ -induced driving force, respectively. Although the bare polarization

diverges logarithmically [6] at  $q_0 = \pm v|\mathbf{q}|$ , this singularity is *cancelled* by the electronic screening of the electron-phonon vertex, which amounts to using the random phase approximation (RPA) expression [21] for  $\Pi(q^2)$ .

The chiral anomaly emerges from  $S_3$ , through the amplitude  $T_{\mu\nu\lambda}$  associated to the ‘‘triangle diagram’’ with two photon and one axial lines [22]. This amplitude has been thoroughly studied in high-energy physics [23], though one important caveat in our case is that Weyl fermions and photons have different phase velocities ( $v$  and  $c$ ). Consequently,  $k^2 = k_0^2 - v^2|\mathbf{k}|^2 = (c^2 - v^2)|\mathbf{k}|^2 \neq 0$  for real photons. It is helpful to decompose  $T_{\alpha\mu\nu}$  into longitudinal and transverse parts [24],

$$T_{\alpha\mu\nu}(k, k') = T_{\alpha\mu\nu}^{(l)}(k, k') + T_{\alpha\mu\nu}^{(t)}(k, k'), \quad (15)$$

such that  $q^\alpha T_{\alpha\mu\nu}^{(l)} \neq 0$  and  $q^\alpha T_{\alpha\mu\nu}^{(t)} = 0$ , where  $q = k + k'$ . The Ward identities  $k^\mu T_{\alpha\mu\nu}^{(l)} = k'^\nu T_{\alpha\mu\nu}^{(l)} = k^\mu T_{\alpha\mu\nu}^{(t)} = k'^\nu T_{\alpha\mu\nu}^{(t)} = 0$  ensure the gauge invariance of  $S_3$ . In particular, the longitudinal part reads

$$T_{\alpha\mu\nu}^{(l)}(k, k') = w_L(q^2) q_\alpha \epsilon_{\mu\nu\rho\sigma} k'^\rho k^\sigma, \quad (16)$$

where  $\epsilon_{\mu\nu\rho\sigma}$  is the Levi-Civita tensor and  $w_L = -i/(2\pi^2 q^2)$ . The *infrared* ( $1/q^2$ ) pole in  $w_L$  is the essence of the chiral anomaly. The transverse part, more complicated, does not contribute to the chiral anomaly, but does contribute to the phonon dynamics and can cancel the  $1/q^2$  pole of  $T^{(l)}$  when either  $k^2$  or  $k'^2$  are nonzero [24].

The analysis becomes remarkably simple when the following conditions are satisfied: (i)  $\mathbf{q} \times \mathbf{g}_0 = 0$ , (ii) the magnetic field contains a dominant constant and uniform part  $\mathbf{B}_0$ , but (iii) the electric field does not. In this case, the contribution of  $T^{(t)}$  is negligible and

$$S_3 = - \sum_{\mathbf{q}\lambda} \int \frac{dq_0}{2\pi} \sqrt{N} v_{\mathbf{q}\lambda}(q_0) \left[ \mathbf{Q}'_{\mathbf{q}\lambda}(1)(q_0) \cdot \mathbf{E}_{-\mathbf{q}}(-q_0) + v \mathbf{Q}'_{\mathbf{q}\lambda}(2)(q_0) \cdot \mathbf{B}_{-\mathbf{q}}(-q_0) + \delta \mathbf{Q}_{\mathbf{q}\lambda}(q_0) \cdot \mathbf{E}_{-\mathbf{q}}(-q_0) \right], \quad (17)$$

where

$$\begin{aligned} \mathbf{Q}'_{-\mathbf{q}\lambda}(1)(-q_0) &= - \frac{e\mathcal{V}}{\pi^2 \hbar^2 v^2 \sqrt{N}} b^\mu \frac{\partial}{\partial q_\mu} \frac{\partial(v\mathbf{q} \times \mathbf{g}_z)}{\partial v_{\mathbf{q}\lambda}(q_0)} \\ \mathbf{Q}'_{-\mathbf{q}\lambda}(2)(-q_0) &= - \frac{e\mathcal{V}}{\pi^2 \hbar^2 v^2 \sqrt{N}} b^\mu \frac{\partial}{\partial q_\mu} \frac{\partial(q_0 \mathbf{g}_z - v\mathbf{q} g_{00})}{\partial v_{\mathbf{q}\lambda}(q_0)} \\ \delta \mathbf{Q}_{-\mathbf{q}\lambda}(q_0) &= \frac{ie^2 \mathcal{V}}{\pi^2 \hbar^2 \sqrt{N}} \frac{\mathbf{B}_0}{q^2} \frac{\partial(q_0 g_{0z} - v\mathbf{q} \cdot \mathbf{g}_0)}{\partial v_{\mathbf{q}\lambda}(q_0)}. \end{aligned} \quad (18)$$

The first and second lines in Eq. (18) originate from the constant part of the axial vector field. The third line in Eq. (18) is special in that it originates from axial electron-phonon interactions ( $g_{0z}$ ,  $\mathbf{g}_0$ ) and constitutes a magnetic-field-induced contribution to the effective charge vector of mode  $\lambda$ . The factor  $i(q_0 g_{0z} - v\mathbf{q} \cdot \mathbf{g}_0)/q^2$  therein can be interpreted as a phonon-induced dynamical axion field.

According to group theory, phonons that are IR inactive at  $\mathbf{B} = 0$  ( $\mathbf{Q}^{(0)} = 0$ ) may become IR active at  $\mathbf{B} \neq 0$  ( $\delta \mathbf{Q} \neq 0$ ), provided that they belong to the direct product of axial and polar irreps [25]. This is indeed the case for  $A_1$  phonons of point groups  $O(432)$  and  $D_3(32)$ , to which belong  $\text{SiSr}_2$  and trigonal  $\text{Te/Se}$ , respectively [26]. However, magnetically induced effective phonon charges are not unique to WSM: they also occur e.g. in multiferroic materials [27]. What is unique about WSM is the mechanism for the  $\mathbf{B}$ -induced IR activity (axial electron-phonon coupling) and the fact that  $\delta \mathbf{Q}$  contains a resonance at  $q_0 = \pm v|\mathbf{q}|$ , due to the chiral anomaly. This resonance is not cancelled by electronic screening of the electron-phonon vertex, because  $1/q^2$  diverges faster than  $1/\log(q^2)$ . Yet, it is crucial that the  $\mathbf{B}$ -field have a nonzero static and uniform component; otherwise the resonance would get cancelled by  $T^{(t)}$ .

In order to assess the observability of our predictions, we estimate  $\delta Q$ . In a TR symmetric and enantiomorphic WSM, we have

$$\frac{|\delta Q_{\mathbf{q}}(q_0)|}{e} \sim \frac{I_0}{\hbar q_0} \frac{q_0^2}{q_0^2 - v^2 \mathbf{q}^2} \frac{B_0 \mathcal{V}_c / a_B}{\phi_0} \frac{b_0}{W}, \quad (19)$$

where  $a_B$  is the Bohr radius,  $I_0$  is a Rydberg,  $\mathcal{V}_c$  is the unit cell volume,  $\phi_0$  is the quantum of flux and  $W \sim O(\Lambda)$  is a characteristic electronic bandwidth. In this estimate, we have assumed that the spatial range of  $\partial_{\mathbf{R}} U(\mathbf{r} - \mathbf{R})$  is about a unit cell, and that its magnitude within that range is about  $I_0/a_B$ . For  $|\mathbf{B}_0| \sim 1\text{T}$ ,  $\mathcal{V}_c \sim 125 \text{\AA}^3$ ,  $I_0/(\hbar q_0) \sim 10^3$  and  $b_0/W \sim 0.1$ , we have  $|\delta Q|/e \sim 0.1/(1 - v^2|\mathbf{q}|^2/q_0^2)$ , which is not negligible (especially close to resonance).

Combining Eqs. (2), (13) and (17), the new equation of motion for the phonons reads

$$\begin{aligned} M(q_0^2 - \omega_{\mathbf{q}\lambda}^2) v_{\mathbf{q}\lambda}(q_0) &= \sqrt{N} \mathbf{Q}_{-\mathbf{q}\lambda}(-q_0) \cdot \mathbf{E}_{\mathbf{q}}(q_0) \\ &+ v \sqrt{N} \left[ \mathbf{Q}_{-\mathbf{q}\lambda}^{(2)}(-q_0) + \mathbf{Q}_{-\mathbf{q}\lambda}^{(2)}(-q_0) \right] \cdot \mathbf{B}_{\mathbf{q}}(q_0), \end{aligned} \quad (20)$$

where  $\mathbf{Q} = \mathbf{Q}^{(0)} + \mathbf{Q}^{(1)} + \mathbf{Q}'^{(1)} + \delta \mathbf{Q}$  and all charges satisfy  $\mathbf{Q}_{-\mathbf{q}} = \mathbf{Q}_{\mathbf{q}}^*$ . Thus, the axial electron-phonon interaction produces a driving force, whose magnitude depends on the relative orientation between  $\mathbf{E}$  and  $\mathbf{B}_0$ . Next, we investigate the physical consequences of the anomaly-induced effective phonon charge.

*Infrared absorption.* – From Eq. (20), the lattice contribution to the dielectric susceptibility reads [14]

$$\chi_{jj'}^{\text{latt}}(\mathbf{q}, q_0) = \frac{1}{M\mathcal{V}_c} \sum_{\lambda} \frac{Q_{\mathbf{q}\lambda j} Q_{-\mathbf{q}\lambda j'}}{(\omega_{\mathbf{q}\lambda}^2 - q_0^2)}, \quad (21)$$

where  $j, j' \in \{x, y, z\}$ . Thus, a constant and uniform magnetic field will induce an IR absorption for the  $A_1$  phonons in a WSM with axial electron-phonon coupling. This is not *per se* a smoking gun of the chiral anomaly, though the fact that  $\delta Q$  has a  $1/q^2$  singularity

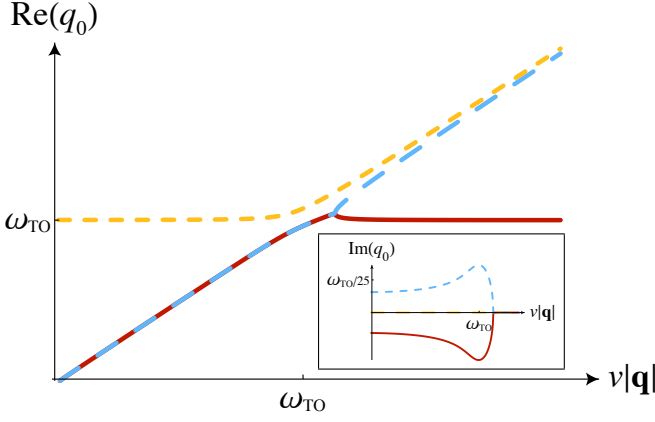


FIG. 1: Anomaly-induced hybridization of a transverse optical phonon ( $\omega_{\mathbf{q}\lambda} = \omega_{\text{TO}} = \text{const}$ ) and a linearly dispersing pseudoscalar boson in presence of a static and uniform magnetic field  $\mathbf{B}_0$  (cf. Eq. (25)). When  $|\mathbf{q}| < \omega_{\text{TO}}/v$ , the linear mode is doubly degenerate but one solution is unstable (anti-damped). A large static dielectric constant is assumed so that Landau damping at  $q_0 > v|\mathbf{q}|$  can be neglected. When  $\mathbf{B}_0 \cdot \hat{\mathbf{q}} = 0$ , the only solution is  $q_0 = \omega_{\text{TO}}$ .

at  $q_0 = v|\mathbf{q}|$  is. Yet, in optical experiments  $q_0 = c|\mathbf{q}|$  and hence the resonance in  $\delta Q$  is not accessible. Alternative probes (inelastic X-ray scattering, electron energy loss spectroscopy) may allow to access the most interesting regime ( $q_0 \simeq \omega_{\mathbf{q}\lambda}$  and  $|\mathbf{q}| \simeq \omega_{\mathbf{q}\lambda}/v$ ). Experimentally, the resonance in  $\delta Q$  may be distinguished from that of the RPA dielectric function because it depends on  $\mathbf{B}$  and it is stronger than logarithmic.

*Raman scattering.*— For IR inactive phonons, the amplitude of Raman scattering is proportional to a triangle diagram with two photon lines and one phonon line [28]. If the dynamical part of  $a^\mu$  is nonzero, this diagram contains an anomalous part given by  $T_{\mu\nu\alpha}$ , thus creating a mathematical link between anomalous quantum breaking of symmetries and Raman spectroscopy. The corresponding “axial” part of the Raman tensor for the  $\lambda$  mode is

$$R_{jj'\lambda}^{\text{ax}} \propto T_{\alpha\mu\nu}(k, k') \frac{\partial^3 [a^\alpha(q)A^\mu(k)A^\nu(k')]}{\partial \mathbf{E}_j(k) \partial \mathbf{E}_{j'}(k') \partial v_{\mathbf{q}\lambda}(q)}, \quad (22)$$

where  $j, j' \in \{x, y, z\}$  denote the directions of the incoming and scattered electric fields  $\mathbf{E}(k)$  and  $\mathbf{E}(k')$ , respectively,  $k = -(\omega, v\mathbf{k})$  and  $k' = (\omega', v\mathbf{k}')$  are the momenta of incoming and scattered photons, and  $q = k + k' = (\omega_{\mathbf{q}\lambda}, v\mathbf{q})$  is the phonon frequency and momentum. Physically, Eq. (22) describes the contribution to the Raman tensor coming from phonon modulations of the *magneto-electric* polarizability. Because  $k$  and  $k'$  are in the infrared, the  $1/q^2$  pole in  $T^{(l)}$  is cancelled by  $T^{(t)}$ . However,

a weaker singularity remains,

$$R_{jj'\lambda}^{\text{ax}} \Big|_{q^2 \simeq 0} \propto \frac{\partial (q_0 g_{0z} - v\mathbf{q} \cdot \mathbf{g}_0)}{\partial v_{\mathbf{q}\lambda}(q_0)} \frac{1}{(k^2 - k'^2)^3} \left[ k^4 \ln \left( \frac{k^2}{q^2} \right) - k'^4 \ln \left( \frac{k'^2}{q^2} \right) \right] \epsilon_{jj'l} (\hat{\mathbf{k}}' - \hat{\mathbf{k}})_l, \quad (23)$$

where  $l \in \{x, y, z\}$  and  $\epsilon_{jj'l}$  is the Levi-Civita tensor. Aside from being antisymmetric under  $j \leftrightarrow j'$  (which is striking for  $A_1$  phonons),  $R_{jj'\lambda}^{\text{ax}}$  contains a logarithmic resonance that is independent from the ultraviolet cut-off of the theory, i.e. associated to low-energy universal properties of 3D Dirac fermions. Moreover, the condition  $q^2 = 0$  is experimentally accessible for optical phonons, because  $\omega_{\mathbf{q}\lambda}/v \simeq 5 \times 10^5 \text{cm}^{-1}$  lies within the range of Raman spectroscopy. Unfortunately, once we incorporate the electronic screening of the electron-phonon vertex, the logarithmic divergence in Eq. (23) is cancelled by a similar singularity in the RPA dielectric function.

The observability of the chiral anomaly in Raman scattering may have better prospects in the case of IR active modes. Let us consider an IR active mode in an enantiomorphic WSM with TR symmetry, e.g. the  $A_1$  mode in SrSi<sub>2</sub>, which is Raman active and becomes IR active when  $\mathbf{B}_0 \neq 0$ . Such a mode creates electric fields that contribute to the Raman scattering [29]. In the electrostatic approximation [30], we write  $\mathbf{E}_{\mathbf{q}} = -i\mathbf{q}\phi_{\mathbf{q}}$ , where  $\phi_{\mathbf{q}}$  is the Fröhlich potential produced by lattice vibrations. To simplify the analysis, we assume low carrier concentrations ( $\omega_{\text{plasma}} \ll \omega_{\mathbf{q}\lambda}$ ), so that the plasmon-phonon hybridization is unimportant. Then, the electric polarization of mode  $\lambda$  in the long wavelength limit is

$$\mathbf{P}_{\mathbf{q}\lambda} = \mathbf{Q}_{\mathbf{q}\lambda} v_{\mathbf{q}\lambda} / (\sqrt{N} \mathcal{V}_c) + (\epsilon_i - 1) \mathbf{E}_{\mathbf{q}} / (4\pi), \quad (24)$$

where  $\epsilon_i(\mathbf{q}, q_0)$  is the contribution of interband electronic transitions to the dielectric function. Combined with Gauss' law, Eq. (24) yields  $\mathbf{E}_{\mathbf{q}} = -\hat{\mathbf{q}} 4\pi \mathbf{Q}_{\mathbf{q}\lambda} \cdot \hat{\mathbf{q}} v_{\mathbf{q}\lambda} / (\sqrt{N} \mathcal{V}_c \epsilon_i)$ . Accordingly, Eq. (20) becomes

$$[q_0^2 - \omega_{\mathbf{q}\lambda}^2 - 4\pi |\mathbf{Q}_{\mathbf{q}\lambda} \cdot \hat{\mathbf{q}}|^2 / (M \mathcal{V}_c \epsilon_i)] v_{\mathbf{q}\lambda} = 0. \quad (25)$$

The solutions of Eq. (25), which in the ordinary case would give the frequency of a longitudinal optical mode, are unusual. As soon as  $\mathbf{B}_0 \cdot \hat{\mathbf{q}} \neq 0$ , a new mode appears due to the anomaly pole, which disperses linearly and hybridizes with the optical phonons at  $q_0 \simeq v|\mathbf{q}|$  (cf. Fig. 1). This extra mode may be the massless and spinless pseudoscalar boson discussed in high-energy physics [31].

In conclusion, we have established a new fingerprint of the chiral anomaly in WSM with axial electron-phonon interactions, which consists of a resonant magnetic-field-induced Born charge for long-wavelength optical phonons. This translates into a magnetic-field-induced infrared activity, as well as a peculiar magnetic-field-dependence of the phonon dispersion.

*Acknowledgements.*— IG acknowledges the hospitality of the Spin Phenomena Interdisciplinary Center

(SPICE), where this work was initiated. We have benefited from fruitful discussion with K. Burch, A. Grushin, D. Pesin and B. Roberge. PR and IG are funded by Québec's RQMP and Canada's NSERC. PLSL is supported by the Canada First Research Excellence Fund.

*Note added.*— After this work was finished and being prepared for submission, we noticed a preprint that overlaps with some of our results, arXiv:1609.05442.

- 
- [1] For reviews, see e.g. P. Hosur and X.-L. Qi, *Comptes Rendus Physique* **14**, 857 (2013); A. A. Burkov, *J. Phys. Condens. Matter* **27**, 113201 (2015).
- [2] A. A. Zyuzin and A. A. Burkov, *Phys. Rev. B* **86**, 115133 (2012).
- [3] S.A. Parameswaran, T. Grover, D.A. Abanin, D.A. Pesin, and A. Vishwanath, *Phys. Rev. X* **4**, 031035 (2014).
- [4] X. Huang, L. Zhao, Y. Long, P. Wang, D. Chen, Z. Hang, H. Liang, M. Xue, H. Weng, Z. Fan, X. Dai and G. Chen, *Phys. Rev. X* **5**, 031023 (2015).
- [5] J. Hutasoit, J. Zang, R. Roiban and C.-X. Liu, *Phys. Rev. B* **90**, 134409 (2014).
- [6] J. Zhou, H.-R. Chang and D. Xiao, *Phys. Rev. B* **91**, 035114 (2015).
- [7] B. Z. Spivak and A. V. Andreev, *Phys. Rev. B* **93**, 085107 (2016);
- [8] I. Garate, *Phys. Rev. Lett.* **110**, 046402 (2013); K. Saha and I. Garate, *Phys. Rev. B* **89**, 205103 (2014); G. Antonius and S. G. Louis, arXiv:1608.00590 (2016); B. Monserrat and D. Vanderbilt, arXiv:1608.00584 (2016)
- [9] K. Saha, K. Légaré and I. Garate, *Phys. Rev. Lett.* **115**, 176405 (2015).
- [10] H. Shapourian, T. L. Hughes and S. Ryu, *Phys. Rev. B* **92**, 165131 (2015).
- [11] A. Cortijo, Y. Ferreira, K. Landsteiner and M. A. H. Vozmediano, *Phys. Rev. Lett.* **115**, 177202 (2015).
- [12] D. I. Pikulin, A. Chen and M. Franz, arXiv:1607.01810 (2016); A. G. Grushin, J. W. F. Venderbos, A. Vishwanath, R. Ilan, arXiv:1607.04268 (2016)
- [13] H. W. Liu, P. Richard, L. X. Zhao, G.-F. Chen and H. Ding, *J. Phys. Cond. Matter* **28**, 295401 (2016); B. Xu et al., arXiv:1608.08160 (2016).
- [14] Yu. A. Il'inskii and L. V. Keldysh, *Electromagnetic Response of Material Media* (Springer, 1984).
- [15] X. Gonze and C. Lee, *Phys. Rev. B* **55**, 10355 (1997).
- [16] See e.g. B. A. Foreman, *J. Phys. Cond. Matter* **12**, R435 (2000).
- [17] S.-M. Huang *et al.*, *Proceedings of the National Academy of Sciences* **113**, 1180 (2016).
- [18] M. Hirayama, R. Okugawa, S. Ishibashi, S. Murakami and T. Miyake, *Phys. Rev. Lett.* **114**, 206401 (2015).
- [19] F. Giustino, arXiv:1603.06965 (2016).
- [20] R. C. Powell, *Symmetry, Group Theory, and the Physical Properties of Crystals* (Springer, New York, 2010).
- [21] H. Bruus and K. Flensberg, *Many-Body Quantum Theory in Condensed Matter Physics: An Introduction* (Oxford, 2004).
- [22] S. L. Adler, *Phys. Rev.* **177**, 2426 (1969); J. Bell and R. Jackiw, *Nuovo Cim.* **A51**, 47 (1969).
- [23] See e.g. R. A. Bertlmann, *Anomalies in quantum field theory* (Clarendon Press, Oxford, 1996).
- [24] R. Armillis, C. Coriano, L. Delle Rose and M. Guzzi, *JHEP* **12**, 029 (2009).
- [25] For a review, see e.g. E. M. Anastassakis in *Dynamical Properties of Solids*, vol. 4, eds. G. K. Horton and A. A. Maradudin (North-Holland, Amsterdam, 1980).
- [26] M. I. Aroyo, J. M. Perez-Mato, D. Orobengoa, E. Tasci, G. de la Flor, A. Kirov; *Bulg. Chem. Commun.* **43** (2), 183 (2011); M. I. Aroyo, J. M. Perez-Mato, C. Capillas, E. Kroumova, S. Ivantchev, G. Madariaga, A. Kirov and H. Wondratschek, *Z. Krist.* **221**, 1 (2006); M. I. Aroyo, A. Kirov, C. Capillas, J. M. Perez-Mato and H. Wondratschek, *Acta Cryst.* **A 62**, 115 (2006); E. Kroumova, M. I. Aroyo, J. M. Perez-Mato, A. Kirov, C. Capillas, S. Ivantchev and H. Wondratschek, *Phase Transitions* **76**, Nos. 1-2, 155 (2003).
- [27] J. Vermette, S. Jandl, M. Orlita, M. M. Gospodinov, *Phys. Rev. B* **85**, 134445 (2012).
- [28] See e.g. A. Pinczuk and E. Burstein, in *Light Scattering in Solids I*, ed. M. Cardona, *Topic in Applied Physics*, vol. 50 (Springer, Berlin, 1982).
- [29] W. D. Johnston, *Phys. Rev. B* **1**, 3494 (1970).
- [30] M. A. Stroschio and M. Dutta, *Phonons in Nanostructures* (Cambridge, UK, 2004).
- [31] M. Gianotti and E. Mottola, *Phys. Rev. D* **79**, 045014 (2009).